

**RESEARCH ARTICLE**

# A three-dimensional model to describe complete human corneal oxygenation during contact lens wear

Marcel Aguilera-Arzo<sup>1</sup> | Vicente Compañ<sup>2</sup>

<sup>1</sup>Department of Physics, Universitat Jaume I, Castellon, Spain

<sup>2</sup>Departamento de Termodinámica Aplicada. Escuela Técnica Superior de Ingenieros Industriales (ETSII), Universitat Politècnica de València, Valencia, Spain

**Correspondence**

Vicente Compañ. Escuela Técnica Superior de Ingenieros Industriales (ETSII), Departamento de Termodinámica Aplicada, Universitat Politècnica de València, C/Camino de Vera s/n. 46020-Valencia, Spain.  
Email: [vicommo@ter.upv.es](mailto:vicommo@ter.upv.es)

**Funding information**

Universitat Jaume I (UJI), Grant/Award Number: UJI-B2018-53

**Abstract**

We perform a novel 3D study to quantify the corneal oxygen consumption and diffusion in each part of the cornea with different contact lens materials. The oxygen profile is calculated as a function of oxygen tension at the cornea-tear interface and the oxygen transmissibility of the lens, with values used in previous studies. We aim to determine the influence of a detailed geometry of the cornea in their modeling compared to previous low dimensional models used in the literature. To this end, a 3-D study based on an axisymmetric volume element analysis model was applied to different contact lenses currently on the market. We have obtained that the model provides a valuable tool for understanding the flux and cornea oxygen profiles through the epithelium, stroma, and endothelium. The most important results are related to the dependence of the oxygen flux through the cornea-lens system on the contact lens thickness and geometry. Both parameters play an important role in the corneal flux and oxygen tension distribution. The decline in oxygen consumption experienced by the cornea takes place just inside the epithelium, where the oxygen tension falls to between 95 and 16 mmHg under open eye conditions, and 30 to 0.3 mmHg under closed eye conditions, depending on the contact lens worn. This helps to understand the physiological response of the corneal tissue under conditions of daily and overnight contact lens wear, and the importance of detailed geometry of the cornea in the modeling of diffusion for oxygen and other species.

**KEYWORDS**

3-D model, corneal oxygen distribution, corneal oxygen flux, Monod kinetics model, oxygen tension, soft contact lens

## 1 | INTRODUCTION

The subject of the oxygen demand of a human cornea has received a great deal of attention in recent years, and has been the subject of an extensive debate, with many models appearing, aiming to explain the distribution of oxygen consumption, the profile of partial pressure of oxygen, and the flux through the entire cornea (epithelium, stroma and endothelium).

Most models carry out their study assuming a 1D geometry for the oxygen transport through the cornea/tear/lens system.<sup>1-6</sup> Some of the models assume a constant thickness and oxygen consumption, and they have evolved considering different multilayers for the cornea/tear/lens system as a mono-dimensional model.<sup>3,4,7-10</sup> However, the first models considered a constant corneal oxygen consumption rate in which the diffusion equation was treated only as steady, and not as time-dependent.<sup>5,11-15</sup> Negative values of the partial pressure

This is an open access article under the terms of the [Creative Commons Attribution-NonCommercial-NoDerivs](https://creativecommons.org/licenses/by-nc-nd/4.0/) License, which permits use and distribution in any medium, provided the original work is properly cited, the use is non-commercial and no modifications or adaptations are made.

© 2022 The Authors. *Journal of Biomedical Materials Research Part B: Applied Biomaterials* published by Wiley Periodicals LLC.

of oxygen in the cornea have frequently been found, which makes no physical sense. In order to resolve this problem, various researchers have created mathematical models based on determination of the oxygen tension at the cornea/tear interface, where the oxygen consumption rate is considered a function of the pressure, and in the majority the researchers have applied the non-linear Monod kinetics model.<sup>16–21</sup> They are all based on knowledge of the values of the partial pressure of oxygen at the cornea-tear interface, determined by the phosphorescence quenching of a dye coated on the rear of a lens.<sup>11,22</sup> This enabled the oxygen tension at the cornea-tear interface to be determined using *in vivo* measurements for different contact lenses worn. However, all the studies carried out have aimed to calculate corneal oxygen consumption have only used the 1-D model. Nevertheless, it is possible to incorporate a three-dimensional study based on an axisymmetric finite element analysis in a realistic model of the equations, as described in this work.

The model presented in this paper is an improvement on the work of Takatori<sup>23</sup> where a complete 3-D treatment with axial symmetry was implemented. In contrast, the model of Takatori et al.<sup>23</sup> and Kim et al.<sup>22</sup> ignores the flow of oxygen in the radial direction, and models all the fluxes, of both oxygen and other species, only through the axial direction. They do this by breaking the system into a series of truncated, concentric spherical sectors. The result is the conversion of the three-dimensional diffusion in an axisymmetric system into a series of approximately equivalent 1-D problems. Unfortunately, this approach makes it very difficult to incorporate possible oxygen flows from the peripheral cornea.

The model presented here allows us to study the influence of oxygen flowing from the limbal region, in line with Takatori's model, and to study a wide variety of lenses thanks to the real-time geometry construction of the system using a few parameters, such as the thickness and oxygen permeability of each lens.

As for the advantages of our work compared to Kim et al.<sup>22</sup> we believe that the model presented by Kim is erroneous in it presents a 2-D diffusion in a section of the eye, but uses Cartesian coordinates, that is, the Kim et al. model uses for the gradient operator the expression ( $\nabla \equiv \frac{\partial}{\partial x}e_x + \frac{\partial}{\partial y}e_y$ ), while in the diffusion equation the term  $\nabla \cdot \vec{J}$  represents a divergence that incorporates an additional radial dependence compared to the Cartesian case (e.g., in the case of interpreting the two directions as those of the cylindrical coordinates). This difference is fundamental; as it incorporates the increase in area of the elements in the radial direction, and this variation is not included a priori in the “rectangular” coordinates (see Appendix A in Kim et al., reference 22).

Finally, in our study we provide a three-dimensional (3-D) study of a cornea as a system of six layers (endothelium-stroma-epithelium/tear/lens/tear), considering that the maximum consumption rate is focused on the epithelium, and it is a function of the oxygen tension at the cornea/tear/lens interface. Accordingly, we determined the corneal oxygen tension and oxygen flux in each part of the cornea (epithelium, stroma and endothelium) during contact lens wear, using data of oxygen tension at the interface epithelium/tear-lens provided by Bonanno et al.<sup>9,11</sup> and determined using the “dye” technique. The oxygen distribution profile

across the cornea is calculated as a function of oxygen permeability of the lens, and the oxygen permeability's values of epithelium, stroma, and endothelium used in previous studies.<sup>14,17,24</sup> This study offers a rigorous and more comprehensive treatment of diffusion in the cornea/tear/lens system by solving 3-D diffusion equations (with axial symmetry) incorporating the possibility of influx of oxygen from the atmosphere through the pericorneal region, and the aqueous humor. The tool allows modeling with only a few input values, under both open eye and closed eye conditions, but still allowing us model a wide range of lenses (material, central and peripheral thickness, optical power, etc.) and corneal geometry. The numerical solution of the transport equations provides a wide range of output values, including oxygen pressure profiles, oxygen fluxes and/or oxygen consumption, as well as integrated values for the various regions of interest in the system, with very small computing requirements, which are available on most current desktop computers. All these parameters are the most important to quantify the corneal physiology for the clinician.

Compared to many previous works, our model includes a rigorous and more comprehensive treatment of diffusion in the cornea/tear/lens system by solving 3-D diffusion equations (with axial symmetry) incorporating the possibility of influx of oxygen from the atmosphere through the pericorneal region and the aqueous humor.

Additionally, all the software used is open source, which makes it much more accessible to any researcher.

## 2 | MATHEMATICAL MODEL

We use FiPy<sup>25</sup> to solve the partial differential equations describing the diffusion of oxygen through the system, as described elsewhere<sup>13,15,24,26,27</sup> and in supplementary information.

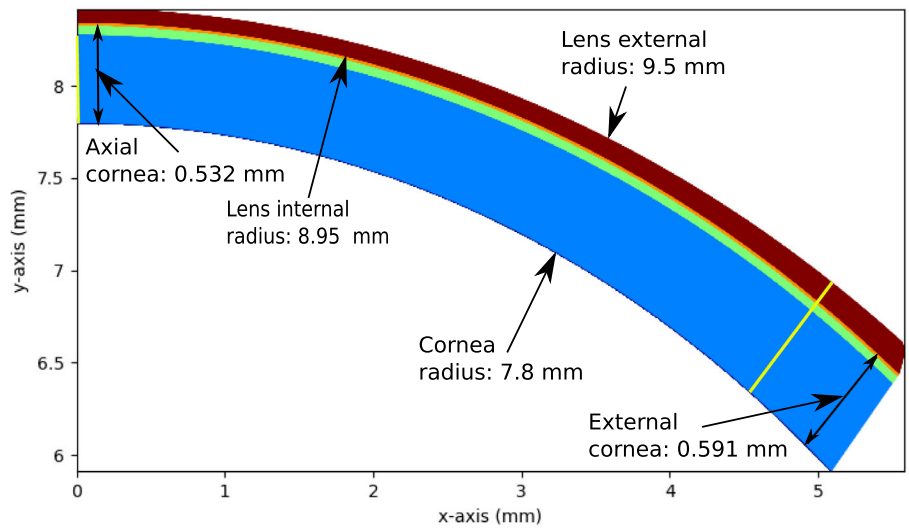
Our model assumes cylindrical symmetry when solving Equation (1), with the axis of symmetry coinciding with the eye axis, but FiPy<sup>25</sup> does not handle this symmetry natively. As a replacement, we used a standard 3D treatment in FiPy, solving for the equation (see supplementary information)

$$rk(\vec{r}) \frac{\partial p(\vec{r}, t)}{\partial t} = \vec{\nabla} \cdot (rk(\vec{r}) D(\vec{r}) \vec{\nabla} p(\vec{r}, t)) - rQ_c(p(\vec{r}, t)) \quad (1)$$

where  $\vec{r} = (r, z)$  are the radial and axial coordinates respectively in our 3D mesh,  $p$  is the partial oxygen pressure,  $k(\vec{r})$  the solubility,  $D(\vec{r})$  the diffusivity,  $Q_c(p(\vec{r}, t))$  is the cornea oxygen consumption and  $t$  is time. Flux computation across different boundaries is needed to incorporate the radial coordinate, as shown in Figure 1.

In this figure, the area highlighted in blue is the stroma, and the area in green is the epithelium. The endothelium area (dark blue) and the tear between the lens and the cornea (light red) and over the lens are barely distinguishable due to their thickness. The lens region used in the simulation is shown in dark red. The lines in yellow are the two axes on which the variation of different quantities is obtained. External and axial thickness for the entire cornea is also shown for this lens with values 591 and 532  $\mu\text{m}$  respectively.

**FIGURE 1** System used for the 3D axisymmetric simulation considering a lens of 71  $\mu\text{m}$  central thickness and  $-3.00$  dioptres



In the second term on the right-hand side in Equation (1) the corneal oxygen consumption  $Q_c(p_c)$  is given as a function of the oxygen partial pressure, which is absent in the contact lens and tear film regions, and follows a Monod kinetics<sup>28,29</sup> form in the corneal system as

$$Q_c(p_c) = \frac{Q_{c,\max} \cdot p(\vec{r}, t)}{K_m + p(\vec{r}, t)} \quad (2)$$

Where,  $Q_{c,\max}$  is the maximum oxygen consumption rate.

In Equations (1) and (2), solubility ( $k(\vec{r})$ ), the diffusion coefficient ( $D(\vec{r})$ ) and the Monod dissociation constant ( $K_m$ ) are considered a function of the position and take constant values within each of the different layers in the system.

Additional details about the model and numerical procedures can be found in the Supplementary Information.

For the geometry generation in FiPy, we used GMSH, as explained in the FiPy manual.<sup>25</sup> GMSH allows us to describe the different eye boundaries as approximate arc segments that can be adjusted in order to approximately represent different cornea/tear/lens systems (see Figure 1).<sup>30</sup> We used around 200 cells in each direction in most of the computations in this study, although this value was checked to ensure good levels of accuracy. All the computations were performed on a personal computer with an Intel Core i7-3770K under Debian Linux. FiPy version 3.1 was used in all the computations. The use of GMSH allows us a great deal of flexibility to describe the geometry. Other methodologies to incorporate the corneal geometry have been proposed in the literature, based on orthogonal polynomials representing the corneal topography.<sup>31,32</sup>

### 3 | PARAMETERS OF THE MODEL

For this study, we selected three contact lenses. The characteristics of the lens, thickness, oxygen permeability, and transmissibility were

measured experimentally in our laboratory, following the procedure described previously (see Table 1 and references 33–35). These values are quite similar to those measured by the manufacturer, which are given in asterisks in Table 1. This table also includes the average maximum oxygen consumption rate estimated previously for the epithelium in a human cornea during contact lens wear.<sup>15,17</sup>

The physiological parameters of the cornea for a 3-D model to calculate the oxygen distribution across the cornea as a function of corneal surface oxygen tension when wearing a contact lens are summarized in Table 2. This table shows the values and units of the considered parameters in our model: oxygen tension on the posterior corneal surface and lens surface under open eye and closed eye conditions. It also presents the values of the maximum oxygen consumption in the endothelium and stroma, oxygen permeability at the epithelium, stroma and endothelium, the tear oxygen permeability, the thicknesses of the epithelium, stroma and endothelium (cornea thickness), the internal and external tear thickness and the metabolic model parameter,  $K_m$ .

The thickness in the cornea increases uniformly from the center, where the thickness is 532  $\mu\text{m}$ , toward the periphery to 591  $\mu\text{m}$  (see Figure 1). The lateral thickness of the stroma and contact lens is considered variable. Each layer has a specific oxygen consumption for the endothelium, stroma and epithelium, according to the values given by Alvord et al.<sup>2</sup> Compañ et al.<sup>14–17</sup> and Larrea et al.<sup>18</sup> respectively. The thicknesses of PoLTF (5  $\mu\text{m}$ ) and PrLTF (15  $\mu\text{m}$ ) are considered constant regardless of the lens worn. The stromal thickness increases as we move away from the eye axis (see Figure 1), as discussed previously by Fares et al.<sup>36</sup> For the oxygen diffusion coefficient in water, we used the value of  $3 \times 10^{-5} \text{ cm}^2/\text{s}$  and for oxygen solubility, the value of  $31 \times 10^{-6} \text{ cm}^3$  of  $\text{O}_2 \text{ cm}^{-3} \text{ mmHg}^{-1}$  measured at 25°C.<sup>37,38</sup> For the partial pressure of oxygen on the posterior corneal surface, we used the value of 24.1 mmHg, which is the aqueous humor oxygen tension used in recent studies.<sup>3,7,22</sup> The oxygen tension on the lens surface under open eye conditions is equal to 155 mmHg, while with closed eyes the value considered for the palpebral conjunctiva is equal to 61.5 mmHg. The permeability values in each layer of the cornea

**TABLE 1** Parameters of the lens used in this study

Lens material (USAN name)	Water content	L ( $\mu\text{m}$ )	P (Barrer)	T (hBarrer/cm)	$Q_{ep}$ , ( $\times 10^{-5}$ ) ( $\text{cm}^3[\text{O}_2] \text{cm}^{-3} \text{s}^{-1}$ )
Galyfilcon A	47%	71 <sup>a</sup>	59.4 (60 <sup>a</sup> )	83.7 (85 <sup>a</sup> )	50.5
Balafilcon A	36%	100 <sup>a</sup>	100.5 (99 <sup>a</sup> )	100.0 (99 <sup>a</sup> )	61
Lotrafilcon A	36%	80 <sup>a</sup>	141.8 (140 <sup>a</sup> )	177.3 (175 <sup>a</sup> )	57

Note: The oxygen permeability and transmissibility of the lenses listed are consistent with those in the paper by L.F. del Castillo et al.<sup>16,17</sup> This table also presents the average maximum consumption ( $Q_{ep}$ ) rate in the epithelium in a human cornea while the soft contact lens specified is worn. 1 Barrer =  $10^{-11}$  ( $\text{cm}^2/\text{s}$ ) ( $\text{ml O}_2 \text{cm}^{-3} \text{mmHg}^{-1}$ ).

<sup>a</sup>Thickness, permeability, and transmissibility are values referred by manufacturer.

**TABLE 2** Parameters considered for the endothelium/stroma/epithelium/internal tear/lens/external tear model system when calculating the oxygen tension distribution and flux profiles through a human cornea when a contact lens is worn

Parameter	Symbol	Value	Units
Partial pressure of oxygen on the posterior corneal surface	$p_{ac}$	24.1	mmHg
Partial pressure of oxygen on the lens surface (open eye)	$p_{air}$	155	mmHg
Partial pressure of oxygen on the lens surface (closed eye) (conjunctiva palpebral)	$P_{cp}$	61.5	mmHg
Maximum endothelium oxygen consumption	$Q_{max,end}$	$47.78 \times 10^{-5}$	$\text{cm}^3(\text{O}_2) \text{cm}^{-3} \text{s}^{-1}$
Maximum stroma oxygen consumption	$Q_{max,es}$	$5.75 \times 10^{-5}$	$\text{cm}^3(\text{O}_2) \text{cm}^{-3} \text{s}^{-1}$
Stroma oxygen permeability	$(DK)_{stroma}$	29.5	Barrer
Endothelium oxygen permeability	$(DK)_{end}$	5.3	Barrer
Epithelium oxygen permeability	$(DK)_{epith}$	18.8	Barrer
Tear (water) oxygen permeability.	$(DK)_{tear}$	93	Barrer
Stroma oxygen diffusion coefficient	$D_{stroma}$	$2.81 \times 10^{-5}$	$\text{cm}^2/\text{s}$
Endothelium oxygen diffusion coefficient	$D_{end}$	$0.496 \times 10^{-5}$	$\text{cm}^2/\text{s}$
Epithelium oxygen diffusion coefficient	$D_{epith}$	$1.767 \times 10^{-5}$	$\text{cm}^2/\text{s}$
Central cornea thickness	CCT	532	$\mu\text{m}$
Central epithelium thickness	$t_{ep}$	50	$\mu\text{m}$
Central stroma thickness	$t_{st}$	480	$\mu\text{m}$
Central endothelium thickness	$t_{en}$	2	$\mu\text{m}$
$K_m$ (metabolic model parameter)	$K_m$	2.2	mmHg
Pre-lens tear thickness (PrLTF)	$t_{lac,in}$	15	$\mu\text{m}$
Post-lens tear thickness (PoLTF)	$t_{lac,ex}$	5	$\mu\text{m}$

Note: 1 Barrer =  $10^{-11}$  ( $\text{cm}^2/\text{s}$ ) ( $\text{ml O}_2 \text{cm}^{-3} \text{mmHg}^{-1}$ ).

were the same as those considered by Alvord et al.<sup>2</sup> The oxygen diffusion coefficients for the epithelium, stroma and endothelium used in this work are the same as those considered by Larrea et al.<sup>18</sup>; the solubility values were therefore calculated based on the permeability values and diffusion coefficient, assuming that average permeability in each layer can be expressed as  $P = Dk$ . Finally, the maximum oxygen consumption rate used in this study was for the endothelium<sup>2</sup> and for the stroma.<sup>18</sup> Based on this assumption, we consider that the largest drop in oxygen tension occurs in the epithelium. Our model therefore assumes that the average consumption in the stroma and endothelium is practically constant, whereas this consumption varies considerably in the epithelium.

## 4 | RESULTS

Figures 2, 3, and 4, for Galyfilcon A, Balafilcon A and Lotrafilcon A lenses shown the results of our 3-D model calculations for the corneal oxygen tension and the oxygen flux module, both under open and closed eye conditions, respectively. Both parameters, oxygen tension and flux module, are plotted for the axis and the periphery of the eye in panels (e) and (f). In addition, we are highlighting the region with zero flux inside the stroma (bright green line through the stroma region in panel [g]). On the other hand, the time-dependent transient oxygen tension (both for closed eye and open eye conditions) on the eye surface axis (blue), and the average oxygen tension on the eye

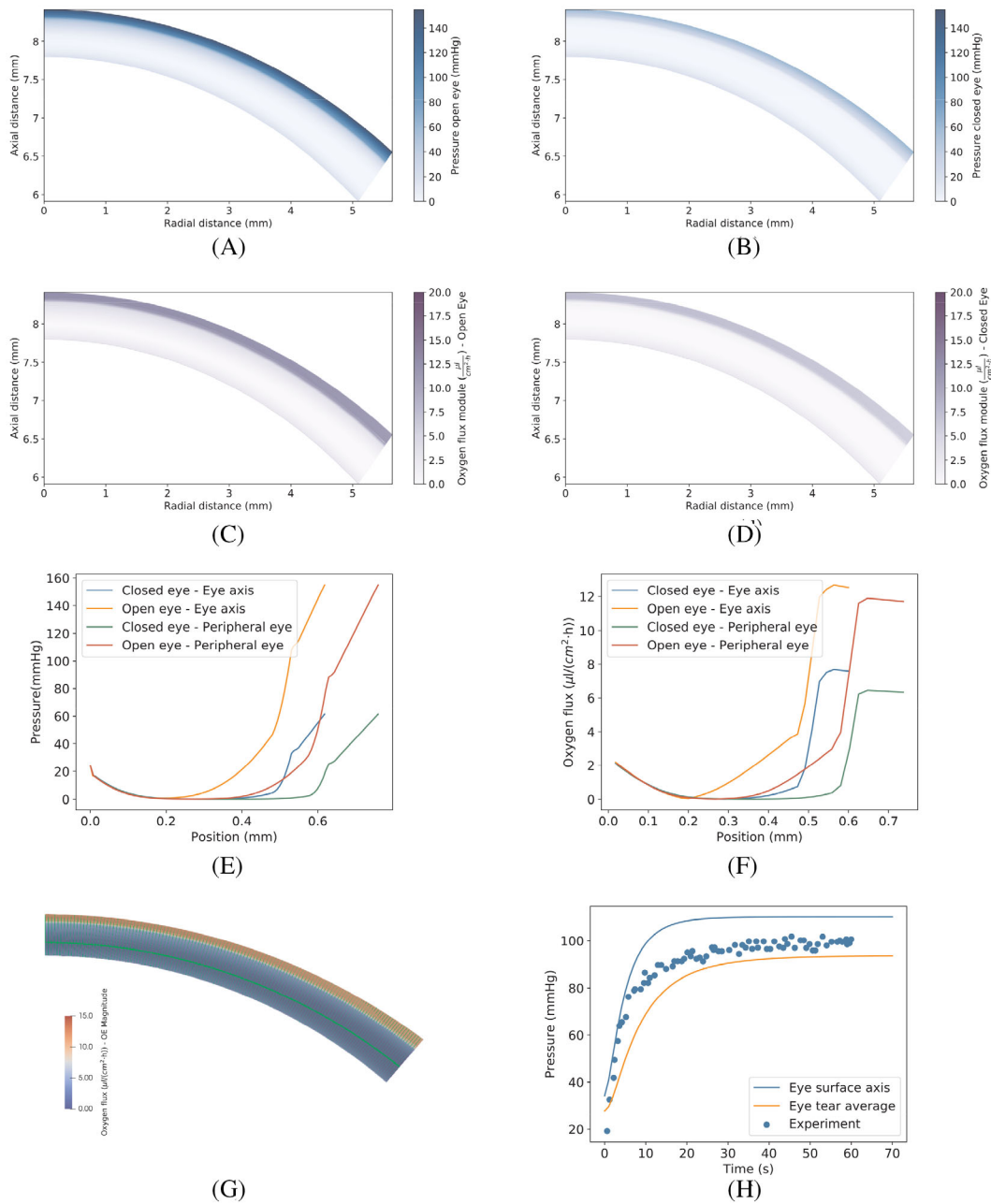


**FIGURE 2** Values for oxygen tension under open (A) and closed (B) eye conditions, oxygen flux module for open (C) and closed eye (D), oxygen tension (E) and oxygen flux module (F) over lines crossing the entire system (yellow paths in Figure 1), lines of oxygen flux (G) and time-dependent transient oxygen tension (H) for a Galyfilcon A lens

tear surface (orange), are shown in Panels (h). Also a comparison with experimental data from Bonnano et al.<sup>19,20</sup> (blue dots) is also shown in the same panel (h).

Figures 2A,B, 3A,B, 4A,B show the results of our 3-D model calculations for a Galyfilcon A, Balafilcon A and Lotrafilcon A lenses of 71, 100 and 80  $\mu\text{m}$  thick (measured in the center of the lens), under open eye conditions (a) and closed eye conditions (b). Under open eye conditions, the pressure in the inner tear region (barely distinguishable in the figure due to its size of 15  $\mu\text{m}$ ) is approximately 100, 118 and

122 mmHg respectively for Galyfilcon A, Balafilcon A and Lotrafilcon A. Also panels (a) clearly show that in the periphery of the system the oxygen tension reaches considerably lower levels than if we stick to the region around the axis of the system (dark blue region), where the oxygen tension reaches an approximate value of 88, 90 and 110 mmHg respectively. Under closed eye conditions, the oxygen tension of the inner tear obtained, varies from 40, 40 and 45 mmHg measured in the center to 25, 25 and 35 mmHg respectively for Galyfilcon A, Balafilcon A and Lotrafilcon A, respectively determined

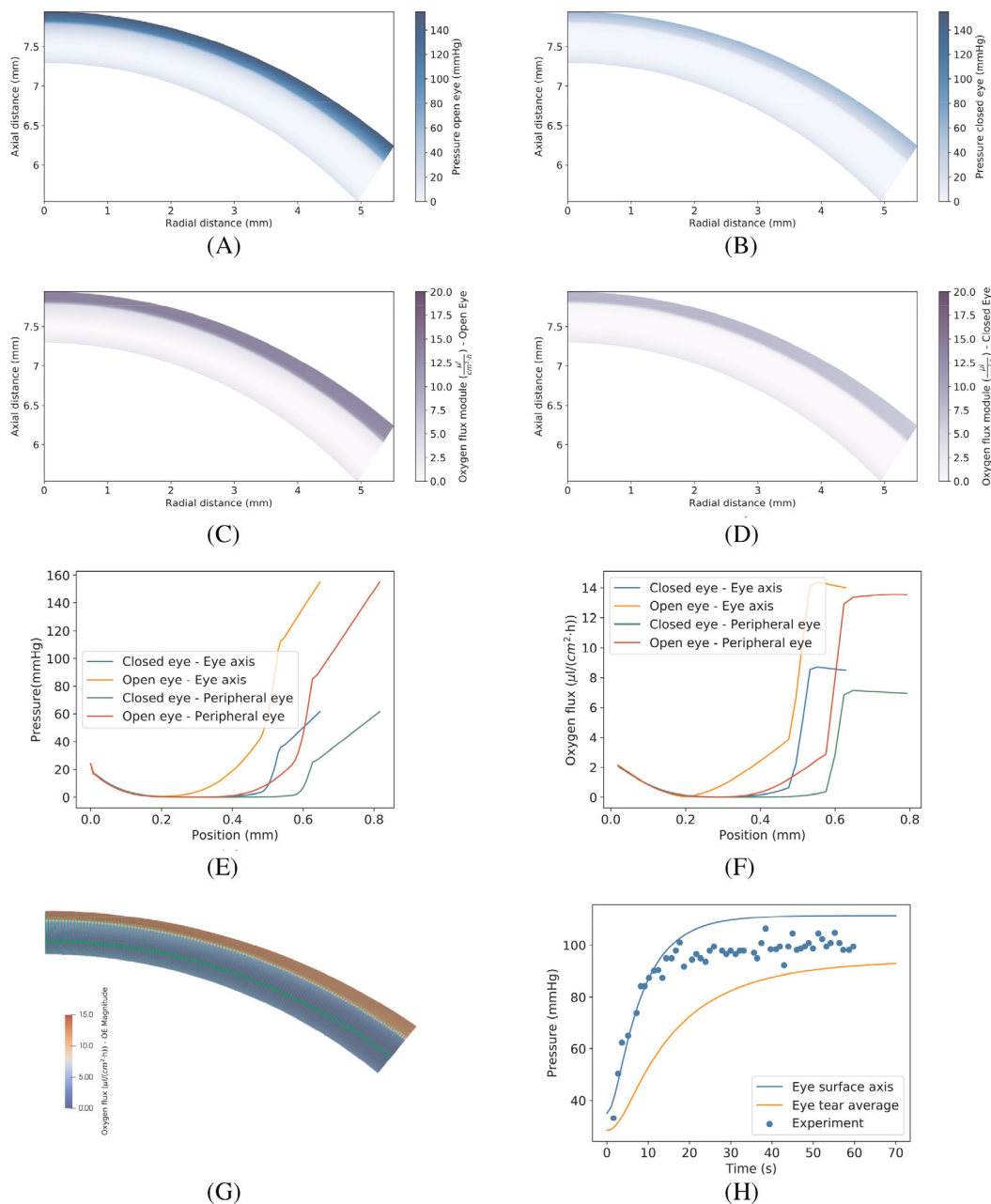


**FIGURE 3** Values for oxygen tension under open (A) and closed (B) eye conditions, oxygen flux module for open (C) and closed eye (D), oxygen tension (E) and oxygen flux module (F) over lines crossing the entire system (yellow paths in Figure 1), lines of oxygen flux (G) and time-dependent transient oxygen tension (H) for a Balafilcon A lens

on the periphery of the system for the lenses used. Note the change of color in Panels (a) and (b) respectively. These values are better determined using Panels (e, f) in Figures 2, 3, and 4.

A similar phenomenon occurs with the oxygen flux through the cornea. Panels (c) and (d) show the magnitude of the oxygen flux under open (c) and closed eye conditions (d) through the different layers of the complete cornea/lens system. In this case, there is a wide region with almost zero oxygen flux, which is the minimum value for the concentration of oxygen (i.e., oxygen partial pressure) in panels (b), which implies that the oxygen supply in this peripheral region mainly comes from the endothelium tissue, while in the region

surrounding the corneal axis the oxygen supply originates through the tear/lens/tear, and comes mainly from the atmosphere. The sharp decrease in oxygen flux module from the tear-epithelium interface toward the stroma is a consequence of the oxygen consumption of the cells in the epithelium layer, as evidenced also in primitive 1D models.<sup>24</sup>

From Figures 2, 3, and 4, we have chosen two lines (in yellow in Figure 1) that go through the lens/tear/cornea system in positions close to the axis of the system (line 1), and another line more on the periphery (line 2), in order to quantify the oxygen pressure gradient under open and closed eye conditions.

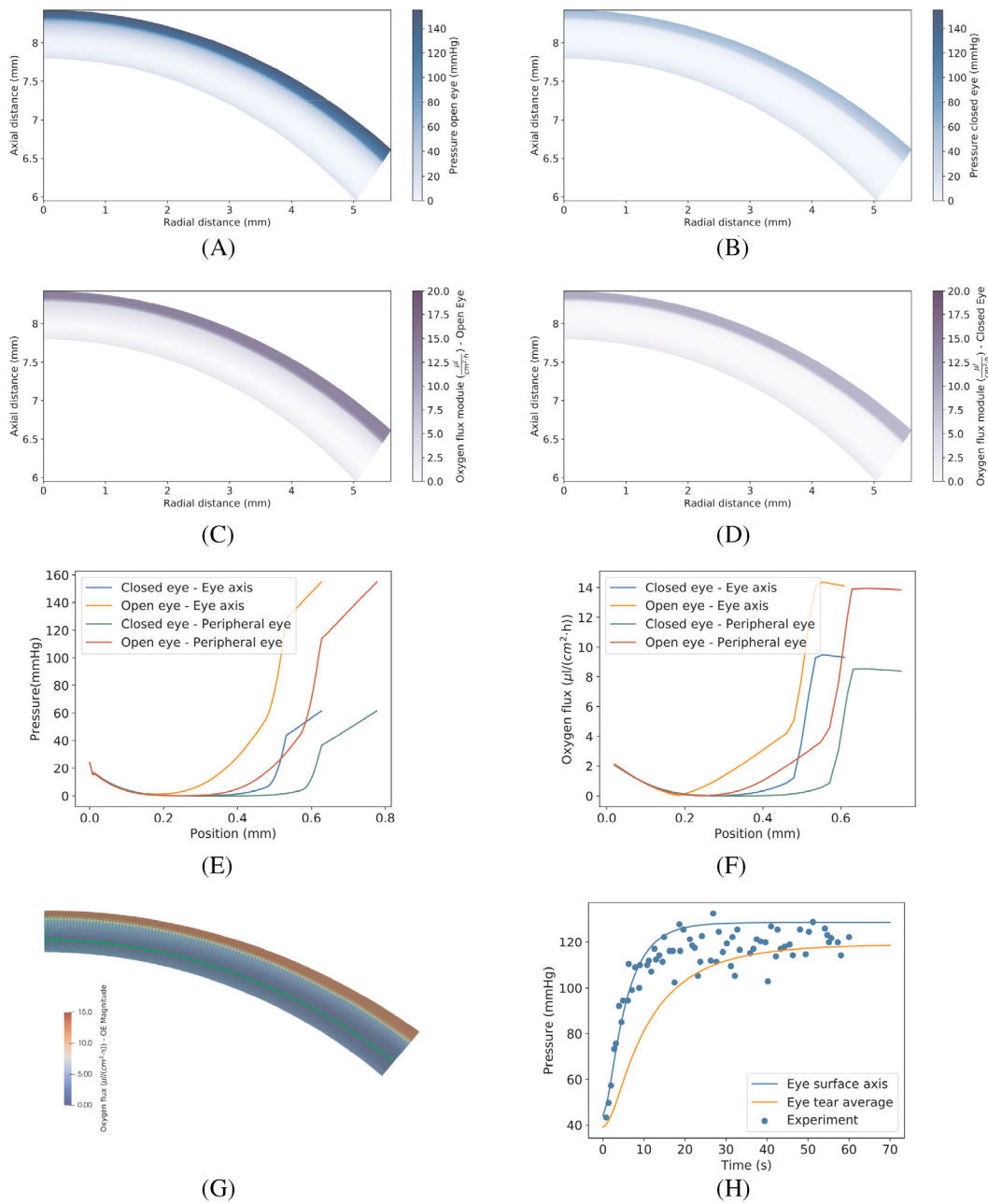


**FIGURE 4** Values for oxygen tension under open (A) and closed (B) eye conditions, oxygen flux module for open (C) and closed eye (D), oxygen tension (E) and oxygen flux module (F) over lines crossing the entire system (yellow paths in Figure 1), lines of oxygen flux (G) and time-dependent transient oxygen tension (H) for a Lotrafilcon A lens

Panels (e) and (f) show the oxygen pressure profiles along the two lines previously selected in this study (axial and peripheral). These figures show how the peripheral line crosses a region with a much lower oxygen concentration, and how this relates to the greater thickness of the cornea in this region. By way of a comparison, it is interesting to consider the result obtained by Compañ et al. using the 1D model for pressure at the cornea-tear interface of 140–150 mmHg.<sup>14,15</sup>

Using the oxygen tensions ( $pO_2$ ) calculated through the cornea-tears-lens, we also calculated the oxygen flux ( $J$ ) using a combination

of Equations (S2) and (S3) and Fick's law of diffusion across each layer. Panels (c) and (d) in Figures 2, 3, and 4 show the oxygen flux profiles for the cornea/tear/lens/tear vault for closed and open eyes respectively. Because there can be no oxygen partial pressure discontinuity at the interfaces between layers (cornea-tears, tears-lens and lens-atmosphere), there must be continuity between fluxes, as was observed in all cases.

A close inspection of panel (c) shows values of the oxygen flux module in the different layers of the system along the two previous lines (being the module the mathematical magnitude of the vector,

in our case the physical oxygen flux, as defined in standard textbooks). This panel also again shows that the values of the fluxes in the periphery are lower than those obtained in the region near the axis, and there is a sharp change in the flow magnitude, which indicates that there is a region in the internal periphery in which the oxygen comes from the epithelium. The oxygen flowing from the exterior lens/tear/cornea together with the oxygen flowing from the endothelium can be seen clearly in Panel (g), which shows the oxygen tension contours under open eye conditions when wearing different lenses as considered in this work, with variable central thickness gathered in Table 1. In this Panel, the green lines show the total oxygen flux into the system from our 3D model. Is very interesting the observation of two regions in the stroma, one with oxygen coming from the outside (from the atmosphere), and another in which the contribution from the endothelium prevails. The dark red regions indicate high oxygen flux, while the dark blue regions indicate low oxygen flux.

The previous results confirm those obtained by other authors and enable an in-depth analysis of the influence of the various parameters on oxygen transport in the lenses under a wide variety of conditions.<sup>2,39</sup>

Our model also allows us also to solve the transient in the same system. To that end, we simulated the evolution of oxygen diffusion from closed eye conditions to open eye conditions considering the same lens-cornea system as before. Panel (e) in Figures 2, 3, and 4 show the oxygen tension profile on the cornea/tear/lens. The major consequence in the simulation is that our 3D model predicts an important difference for the oxygen pressure profile on the cornea-lens interface (or cornea-tear in our model), if the oxygen pressure on the axis is taken as the reference (the blue line in Panels [e]) or the average oxygen pressure on the entire surface of the tear (the orange line in Panels [f]) is used. This is again due to the difference in thickness of the lens in the peripheral zone compared to the central zone, which results in a slower contribution of oxygen from the atmosphere, and therefore in a longer relaxation time in the peripheral region. This confirms that cornea and contact lens thickness variations play an important role in the oxygen flux diffusion, mostly through the epithelium and stroma.

Finally, in Panels (h) the post lens tear-film oxygen tension on the surface of the eye as a function of time has also been plotted, in both the axial position and averaged over the region of the tear between the lens and the surface of the cornea. As is apparent for the cornea/tear/lens system, there is a good fit between the experimental data and the oxygen pressure values in the axial zone, whereas if we take the average for the tear region, the values are somewhat underestimated compared to the experimental values.

The oxygen permeability of the lens causes an increase or decrease in the corneal oxygenation, as seen in the contour plots. For example, a comparison between Figures 2A,B and 3A,B for the Galyfilcon A and Balafilcon A lens, respectively, shows larger central dark blue regions in Galyfilcon A compared to Balafilcon A, spreading inwards from the corneal periphery. Under closed eye conditions, there is a major decline in oxygen concentration across the entire

cornea (endothelium, stroma and epithelium), as shown by the change from dark blue to light blue.

Although it is difficult to distinguish the differences between the Balafilcon A (Figure 3A,B), and Galyfilcon A (Figure 2A,B) lenses with this type of representation, it is possible to observe an increase in the region, with higher oxygen concentration values due to both the higher transmissibility of the Balafilcon A (100.0 hBarrer/cm) lens compared to the Galyfilcon A lens (83.7 hBarrer/cm) (Figure 2A,B), and because of the greater thickness of this lens. In addition, it has slightly higher maximum consumption in the area of the cornea from the endothelium to epithelium through the stroma. This is further shown in the case of Lotrafilcon A (Figure 4A,B): The thickness of the lens is similar to that of the Galyfilcon A lens, but the transmissibility of the Lotrafilcon A lens (177 hBarrer/cm) is considerably greater.

As for the oxygen flux, a comparison between the three lenses suggests that for the Lotrafilcon A lens, higher flow values are observed than for the other two lenses. This is undoubtedly due to the higher transmissibility of this lens (around of 177 hBarrer/cm), combined with similar consumption values in the cornea region, which generally increases the oxygen flows in the system. In general, the transition region between oxygen flow from the endothelium to the oxygen flow from tears is always around 200  $\mu\text{m}$  from the endothelium with open eyes and about 250  $\mu\text{m}$  for closed eyes, taking the axial axis as a reference. The greater consumption of oxygen in the corneal area ( $Q_c$ ) and a higher transmissibility of these lenses could explain this difference.

Table 3 shows values obtained from our 3D model for the oxygen tension, oxygen flux and oxygen consumption at the interfaces Endothelium/Stroma, Stroma/Epithelium and Epithelium/Tear for the three lenses studied, and let us conclude that our model give an estimation of oxygen flux and oxygen tension distribution with values ensuring a good oxygenation for the demands generated in each of its parts (epithelium, stroma and endothelium), both for open and closed eye conditions. The oxygen tension profile suggests that the oxygen flux increases toward the periphery and subsequently declines quickly near the limbus. This happens more sharply in thin lenses. To compare them we also determined the same parameters without a lens on the cornea.

The oxygen consumption in the epithelium using the 3D-model for Galyfilcon A, Balafilcon A and Lotrafilcon A contact lenses shows that under closed eye conditions is  $Q_{\text{Galyf}} (=6.52 \times 10^{-5} \text{ cm}^3 (\text{O}_2) \text{ cm}^{-3} \text{ s}^{-1}) < Q_{\text{Balaf}} (=7.0 \times 10^{-5} \text{ cm}^3 (\text{O}_2) \text{ cm}^{-3} \text{ s}^{-1}) < Q_{\text{Lotraf}} = 7.44 \times 10^{-5} \text{ cm}^3 (\text{O}_2) \text{ cm}^{-3} \text{ s}^{-1})$  when the system is under closed eye conditions. However, under open eye conditions, the trend is  $Q_{\text{Galyf}} (=9.2 \times 10^{-5} \text{ cm}^3 (\text{O}_2) \text{ cm}^{-3} \text{ s}^{-1}) < Q_{\text{Lotraf}} (=10.0 \times 10^{-5} \text{ cm}^3 (\text{O}_2) \text{ cm}^{-3} \text{ s}^{-1}) \cong Q_{\text{Balaf}} (=10.1 \times 10^{-5} \text{ cm}^3 (\text{O}_2) \text{ cm}^{-3} \text{ s}^{-1})$ . A comparison between the values found for the oxygen consumption considering the 1-D (see values in Table S1 of Supplementary Information) and 3-D models, during the night for the three lenses is around of 20% higher in our 3-D model than the study using a 1-D model. This percentage increase for Galyfilcon A lenses even when the comparison is done during the day.



**TABLE 3** Oxygen tension and oxygen flux values at the system interfaces between the internal endothelium/stroma/epithelium/tear and average consumption in each region, under both open and closed eye conditions according to the 3D model

Lens	Quantity	Endothelium/Stroma	Stroma/Epithelium	Epithelium/Tear
Closed eye				
Galyfilcon A	$p$ (mmHg)	21.43	2.88	26.84
	$J$ ( $\mu\text{l}/\text{cm}^2 \text{ h}$ )	2.36	0.55	7.11
	$Q$ ( $\mu\text{l}/\text{cm}^3 \text{ h}$ )	1568.19	58.63	1411.62
Balafilcon A	$p$ (mmHg)	21.43	2.07	27.32
	$J$ ( $\mu\text{l}/\text{cm}^2 \text{ h}$ )	2.36	0.42	8.01
	$Q$ ( $\mu\text{l}/\text{cm}^3 \text{ h}$ )	1568.18	55.85	1639.32
Lotrafilcon A	$p$ (mmHg)	21.43	4.88	37.90
	$J$ ( $\mu\text{l}/\text{cm}^2 \text{ h}$ )	2.36	0.84	9.34
	$Q$ ( $\mu\text{l}/\text{cm}^3 \text{ h}$ )	1568.18	65.89	1732.50
No lens	$p$ (mmHg)	21.44	23.79	59.40
	$J$ ( $\mu\text{l}/\text{cm}^2 \text{ h}$ )	2.35	2.60	7.39
	$Q$ ( $\mu\text{l}/\text{cm}^3 \text{ h}$ )	1568.21	100.79	879.40
Open eye				
Galyfilcon A	$p$ (mmHg)	21.35	34.99	91.92
	$J$ ( $\mu\text{l}/\text{cm}^2 \text{ h}$ )	2.43	3.34	12.80
	$Q$ ( $\mu\text{l}/\text{cm}^3 \text{ h}$ )	1567.94	107.51	1745.10
Balafilcon A	$p$ (mmHg)	21.35	29.91	91.07
	$J$ ( $\mu\text{l}/\text{cm}^2 \text{ h}$ )	2.43	3.05	14.45
	$Q$ ( $\mu\text{l}/\text{cm}^3 \text{ h}$ )	1567.93	102.34	2097.71
Lotrafilcon A	$p$ (mmHg)	21.35	49.48	116.58
	$J$ ( $\mu\text{l}/\text{cm}^2 \text{ h}$ )	2.43	4.08	14.94
	$Q$ ( $\mu\text{l}/\text{cm}^3 \text{ h}$ )	1566.48	184.21	1987.58
No lens	$p$ (mmHg)	21.38	92.20	151.91
	$J$ ( $\mu\text{l}/\text{cm}^2 \text{ h}$ )	2.40	5.69	10.89
	$Q$ ( $\mu\text{l}/\text{cm}^3 \text{ h}$ )	1568.04	151.28	915.20

A comparison between the oxygen consumption found in this study for the three lenses, with an oxygen tension at the epithelium/tear interface higher than 100 mmHg, and the value obtained by Bonanno et al.<sup>11</sup> for similar surface  $P_{\text{O}_2}$ , ( $Q = 22 \times 10^{-5} \text{ cm}^3 (\text{O}_2) \text{ cm}^{-3} \text{ s}^{-1}$ ), shows that this is practically double to the values obtained in our work. For a cornea without a lens, the average oxygen consumption under closed eye conditions was  $4.98 \times 10^{-5} \text{ cm}^3 (\text{O}_2) \text{ cm}^{-3} \text{ s}^{-1}$  and under open eye conditions the value obtained with our 3D model is  $6.3 \times 10^{-5} \text{ cm}^3 (\text{O}_2) \text{ cm}^{-3} \text{ s}^{-1}$ . These values are smaller than those obtained with the 1D model, because the oxygen consumption under open eye conditions was  $7.4 \times 10^{-5} \text{ cm}^3 (\text{O}_2) \text{ cm}^{-3} \text{ s}^{-1}$ , and for closed eye conditions (i.e., during the night) the value was  $6.4 \times 10^{-5} \text{ cm}^3 (\text{O}_2) \text{ cm}^{-3} \text{ s}^{-1}$ .

The oxygen flux found in the epithelium/tear interface was 7.11, 8.01, and  $9.34 \mu\text{l} (\text{O}_2) \text{ cm}^{-3} \text{ h}^{-1}$  for Galyfilcon A, Balafilcon A and Lotrafilcon A respectively under closed eye conditions, while under open eye conditions the oxygen flux was 12.8, 14.45, and  $14.94 \mu\text{l} (\text{O}_2) \text{ cm}^{-3} \text{ h}^{-1}$ , for Galyfilcon A, Balafilcon A and Lotrafilcon A respectively. These values are higher than the values found using a 1D model by Brennan<sup>7</sup> and Del Castillo,<sup>16</sup> who estimated oxygen flux values of around 7.8 and  $6.0 \mu\text{l} (\text{O}_2) \text{ cm}^{-3} \text{ h}^{-1}$  under open eye and closed eye conditions respectively using the diffusion model.<sup>7,16</sup>

Finally, our results estimate an average oxygen consumption rate in the epithelium of around  $3.9 \times 10^{-4}$ ,  $4.5 \times 10^{-4}$  and  $4.7 \times 10^{-4} \mu\text{l} (\text{O}_2) \text{ cm}^{-3} \text{ s}^{-1}$ , for Galyfilcon A, Balafilcon A and Lotrafilcon A respectively under closed eye conditions and  $4.9 \times 10^{-4}$ ,  $5.9 \times 10^{-4}$  and  $5.5 \times 10^{-4} \mu\text{l} (\text{O}_2) \text{ cm}^{-3} \text{ s}^{-1}$ , for Galyfilcon A, Balafilcon A and Lotrafilcon A respectively under open eye conditions. These values are higher than the values used by Alvord et al.<sup>2</sup> as parameters in his 1D model based on the BEL-model, which was  $25.9 \times 10^{-5} \mu\text{l} (\text{O}_2) \text{ cm}^{-3} \text{ s}^{-1}$ , half the values estimated in our 3D model.

Given the different results found in this study for corneal oxygenation between the central and peripheral regions, we expected changes in the different reactions including glucose, lactate ions, bicarbonate ions, carbon dioxide, and hydrogen ions, which take place in the various parts of the cornea (epithelium, stroma and endothelium), as has been reported by various researchers.<sup>1,3,12,19,22,24</sup> A more comprehensive study to determine how to change the carbon dioxide, glucose, bicarbonate and lactate profiles and the change in pH because of the lack of oxygen using our 3D model will be performed in the future.

From the values reported in Table 3, we find that percent oxygen consumption between the different regions of the cornea are approximately 3%, 36%, and 61% respectively for endothelium, stroma and

epithelium wearing a Galyfilcon A lens onto a human cornea. These values are quite similar for Balafilcon A and 2%, 46%, and 52% for Lotrafilcon A. All these values are valid under open eye conditions.

Assuming the ratio of epithelial to endothelial cells is about 7:1, the percent oxygen consumption of the endothelium cells is approximately 6.3 that of epithelium cells when a Galyfilcon A lens is used, according to our model. Corresponding values of 5.2 and 5.5 are found in case of Balafilcon A and Lotrafilcon A lenses. This study highlights the excellent and equivalent oxygen performance of Galyfilcon A and Balafilcon A during use prolonged, but its performance are smaller than Lotrafilcon A. In summary, material selection seems to be critical for maintaining corneal health, to guarantee that there is sufficient oxygen to maintain a good corneal physiology the material configuring the CL should have at least 80 hBarrer/cm of transmissibility. From these results, we think the combination of this model with tear film oxygen tension measurements given by the performance of a CL can be useful to predict that maximum hypoxic corneal stress ( $S_{\text{min}}$ ) moves from close to the endothelium toward the anterior stroma, and both deepens and broadens as anterior corneal surface oxygen tension decrease. On the other hand, 3D model predicts sufficient oxygen flux through epithelium in the three SiH materials studied.

This work is limited to the diffusion and consumption of oxygen in each part of the cornea (epithelium, stroma, and endothelium). We think that a more rigorous approach should also include studies of carbon dioxide, glucose, lactate ion, hydrogen ion, bicarbonate ion, sodium ion, and chloride ion, in addition to water hydration and pressure. The knowledge of the parameters would give a complete picture that explains how epithelial hypoxia induces corneal edema.

## 5 | CONCLUSIONS

In this work, we have solved the non-stationary equations describing the oxygen transport through the cornea-lens systems by using a 3D model with axial symmetry. Our model, though not completely realistic, approximate the cornea-system by using only a few set of parameters (corneal and/or lens curvature radius, center of curvature, lens permeability ...) which allows us to describe several lenses of commercial interest.

We have found that the corneal oxygen demand is not constant over the entire surface of the cornea. Previous 1D models considered only the center of the cornea and contact lens. This would lead to anoxia in limbal regions of the cornea.

The results for oxygen tension in the region of the periphery are lower than the axial region due to the greater thickness of the cornea and lens in this area in the lenses modeled in this work. Cornea and contact lens thickness variations play an important role in the corneal flux and oxygen tension distribution, for which a significant effect on the oxygen availability is observed.

The cornea is divided into two regions so that the flow of oxygen in each one comes from the inside of the cornea (the aqueous humor), or from the exterior of the cornea/tear/lens from the atmospheric oxygen tension. These two regions are separated by a surface, which

is the equivalent to the point of maximum oxygen corneal stress in 1D models<sup>14</sup> ( $x_{\text{min}}$ ). This surface can be defined both as the points of minimum oxygen tension or the points of zero oxygen flux (green line in panel h of Figures 2 to 4). As in the case of the 1D model,<sup>14</sup> it is found that the position of this surface depends on the pressure at the surface of the cornea, so that it is displaced from close to the endothelium toward the anterior stroma, and both deepens and broadens as anterior corneal surface oxygen tension decreases (that is, from open to closed eye conditions).

The 3-D model under open eye conditions suggest an anterior corneal oxygen tension, flux and an oxygen distribution in the epithelial tissue in contact with the tear of 92 mmHg, 12.8  $\mu\text{l}/\text{cm}^2$  h and  $4.83 \times 10^{-4}$   $\text{ml}(\text{O}_2)/\text{cm}^3$  s respectively when the Galyfilcon A contact lens is worn. The decline in oxygen consumption supported by the cornea takes place just inside the epithelium, where the oxygen tension declines by between 155 and 116 for the Lotrafilcon A lens and 155 to 91 mmHg for Balafilcon A under open eye conditions. However, this decline under closed eye conditions was from 61.5 to 37.9 for Lotrafilcon A, while it was from 64.5 to 16.8 mmHg for Galyfilcon A.

This work shows that proper inclusion of the realistic geometry of the Cornea-Lens systems is of utmost importance in order to obtain realistic values of oxygen tension, flux, and consumption for a set of commercially available lenses present in the market.

Our model estimate an average oxygen consumption rate in the epithelium of around  $3.9 \times 10^{-4}$ ,  $4.5 \times 10^{-4}$  and  $4.7 \times 10^{-4}$   $\mu\text{l}(\text{O}_2) \text{cm}^{-3} \text{s}^{-1}$ , for Galyfilcon A, Balafilcon A and Lotrafilcon A respectively under closed eye conditions and  $4.9 \times 10^{-4}$ ,  $5.9 \times 10^{-4}$  and  $5.5 \times 10^{-4}$   $\mu\text{l}(\text{O}_2) \text{cm}^{-3} \text{s}^{-1}$ , for Galyfilcon A, Balafilcon A and Lotrafilcon A, respectively under open eye conditions. On the other hand, the variation of oxygen flux between the interfaces epithelium/tear and stroma/epithelium are found to be supported to a surface  $\text{PO}_2$  range of 57 mmHg, 61 and 67 mmHg, for Galyfilcon A, Balafilcon A and Lotrafilcon A, respectively. Taking into account values obtained from 1D model<sup>14</sup> we can conclude that following our 3D model none of these three lenses provide critical oxygen flux and oxygen tension values capable of producing hypoxia-induced corneal swelling.

Additionally we have solved for the full time-dependent diffusion equation, not only the steady-state equation as previous works,<sup>2,22,23</sup> which permits us to compare the transient oxygen tension at the surface of the eye (see panel "h" in Figures 2, 3 and 4) with experimental data, further validating our approach.

## AUTHOR CONTRIBUTIONS

Conceptualization, Marcel Aguilera-Arzo and Vicente Compañ; investigation, Marcel Aguilera-Arzo and Vicente Compañ; writing—original draft preparation, Marcel Aguilera-Arzo and Vicente Compañ; writing—review and editing, Marcel Aguilera-Arzo and Vicente Compañ; supervision, Marcel Aguilera-Arzo and Vicente Compañ; project administration, Marcel Aguilera-Arzo and Vicente Compañ; funding acquisition, Marcel Aguilera-Arzo and Vicente Compañ. All the authors contributed to the discussions. All authors have read and agreed to the published version of the manuscript.

## ACKNOWLEDGMENTS

This research was funded by the Universitat Jaume I (UJI) under the project UJI-B2018-53. We thanks to Robert Jones for the English language revision.

## CONFLICT OF INTEREST

The authors declare no conflicts of interest.

## DATA AVAILABILITY STATEMENT

The data of our findings are available from the corresponding author upon reasonable request.

## REFERENCES

- Leung BK, Bonanno JA, Radke CJ. Oxygen-deficient metabolism and corneal edema. *Prog Retin Eye Res.* 2011;30:471-492.
- Alvord LA, Hall WJ, Keyes LD, Morgan CF, Winterton LC. Corneal oxygen distribution with contact lens wear. *Cornea.* 2007;26:654-664.
- Fatt I, Bieber MT. The steady-state distribution of oxygen and carbon dioxide in the in vivo cornea. I. the open eye in air and the closed eye. *Exp Eye Res.* 1968;7:103-112.
- Fatt I, Freeman RD, Lin D. Oxygen tension distributions in the cornea: a Re-examination. *Exp Eye Res.* 1974;18:357-365.
- Fatt I. Steady-state distribution of oxygen and carbon dioxide in the in vivo cornea. II. the open eye in nitrogen and the covered eye. *Exp Eye Res.* 1968;7:413-430.
- Brennan NA. Corneal oxygenation during contact lens wear: comparison of diffusion and EOP-based flux models. *Clin Exp Optom.* 2005;88:103-108.
- Brennan NA. Beyond flux: total corneal oxygen consumption as an index of corneal oxygenation during contact lens wear. *Optom Vis Sci.* 2005;82:467-472.
- Fatt I, Weissman BA. The lens. *Physiology of the Eye.* Elsevier; 1992:85-95.
- Harvitt DM, Bonanno JA. Re-evaluation of the oxygen diffusion model for predicting minimum contact lens Dk/t values needed to avoid corneal anoxia. *Optom Vis Sci.* 1999;76:712-719.
- Freeman RD. Oxygen consumption by the component layers of the cornea. *J Physiol.* 1972;225:15-32.
- Bonanno JA, Stickel T, Nguyen T, et al. Estimation of human corneal oxygen consumption by noninvasive measurement of tear oxygen tension while wearing hydrogel lenses. *Invest Ophthalmol Vis Sci.* 2002;43:371-376.
- Fatt I, Bieber MT, Pye SD. Steady state distribution of oxygen and carbon dioxide in the in vivo cornea of an eye covered by a gas-permeable contact lens. *Am J Optom Arch Am Acad Optom.* 1969;46:3-14.
- Compañ V, Aguilera-Arzo M, Del Castillo LF, et al. Analysis of the application of the generalized Monod kinetics model to describe the human corneal oxygen-consumption rate during soft contact lens wear. *J Biomed Mater Res B Appl Biomater.* 2017;105:2269-2281.
- Compañ V, Aguilera-Arzo M, Weissman BA. Corneal equilibrium flux as a function of corneal surface oxygen tension. *Optom Vis Sci.* 2017;94:672-679.
- Compañ V, Aguilera-Arzo M, Edrington TB, Weissman BA. Modeling corneal oxygen with scleral gas permeable lens wear. *Optom Vis Sci.* 2016;93:1339-1348.
- Del Castillo LF, da Silva ARF, Hernández SI, et al. Diffusion and Monod kinetics model to determine in vivo human corneal oxygen-consumption rate during soft contact lens wear. *J Optom.* 2015;8:12-18.
- Del Castillo LF, Ramírez-Calderón JG, Del Castillo RM, et al. Corneal relaxation time estimation as a function of tear oxygen tension in human cornea during contact lens wear. *J Biomed Mater Res B Appl Biomater.* 2020;108:14-21.
- Larrea X, Büchler P. A transient diffusion model of the cornea for the assessment of oxygen diffusivity and consumption. *Invest Ophthalmol Vis Sci.* 2009;50:1076-1080.
- Bonanno JA, Clark C, Pruitt J, Alvord L. Tear oxygen under hydrogel and silicone hydrogel contact lenses in humans. *Optom Vis Sci.* 2009;86:E936-E942.
- Masters BR. Direct noninvasive measurement of tear oxygen tension beneath gas-permeable contact lenses in rabbits. *Invest Ophthalmol Vis Sci.* 1996;37:1935.
- Takatori SC, de la Jara PL, Holden B, Ehrmann K, Ho A, Radke CJ. In vivo oxygen uptake into the human cornea. *Invest Ophthalmol Vis Sci.* 2012;53:6331-6337.
- Kim YH, Lin MC, Radke CJ. Limbal metabolic support reduces peripheral corneal edema with contact-lens wear. *Transl Vis Sci Technol.* 2020;9:44.
- Takatori SC, Radke CJ. A Quasi-2-dimensional model for respiration of the cornea with soft contact lens wear. *Cornea.* 2012;31:405-417.
- Compañ V, Aguilera-Arzo M, del Castillo RM, et al. A refined model on flow and oxygen consumption in the human cornea depending on the oxygen tension at the Interface cornea/post lens tear film during contact lens wear. *J Optom.* 2022;15:160-174.
- Guyer JE, Wheeler D, Warren JA. FiPy: partial differential equations with python. *Comput Sci Eng.* 2009;11:6-15.
- Compañ V, Aguilera-Arzo M, Montero AE, et al. Comments to paper entitled: predicting scleral GP lens entrapped tear layer oxygen tensions. *Cont Lens Anterior Eye.* 2015;38:391.
- Compañ V, Oliveira C, Aguilera-Arzo M, Mollá S, Peixoto-de-Matos SC, González-Méijome JM. Oxygen diffusion and edema with modern scleral rigid gas permeable contact lenses. *Invest Ophthalmol Vis Sci.* 2014;55:6421-6429.
- Chhabra M, Prausnitz JM, Radke CJ. Modeling corneal metabolism and oxygen transport during contact lens wear. *Optom Vis Sci.* 2009;86:454-466.
- Chhabra M, Prausnitz JM, Radke CJ. Diffusion and Monod kinetics to determine in vivo human corneal oxygen-consumption rate during soft contact-lens wear. *J Biomed Mater Res B Appl Biomater.* 2009;90:202-209.
- Geuzaine C, Remacle J-F. Gmsh: a 3-D finite element mesh generator with built-in pre- and post-processing facilities. *Int J Numer Methods Eng.* 2009;79:1309-1331.
- Wang J, Li X, Wang Z, et al. Accuracy and reliability of orthogonal polynomials in representing corneal topography. *Med Nov Technol Devices.* 2022;15:100133.
- Talu S, Talu M. An overview on mathematical models of human corneal surface. *IFMBE Proc.* 2009;26:291-294.
- Compañ V, Andrio A, López-Aleman A, Riande E, Refojo MF. Oxygen permeability of hydrogel contact lenses with organosilicon moieties. *Biomaterials.* 2002;23:2767-2772.
- Gonzalez-Mejome JM, Compañ-Moreno V, Riande E. Determination of oxygen permeability in soft contact lenses using a polarographic method: estimation of relevant physiological parameters. *Ind Eng Chem Res.* 2008;47:3619-3629.
- Gavara R, Compañ V. Oxygen, water, and sodium chloride transport in soft contact lenses materials. *J Biomed Mater Res B Appl Biomater.* 2017;105:2218-2231.

36. Fares U, Otri AM, Al-Aqaba MA, Dua HS. Correlation of central and peripheral corneal thickness in healthy corneas. *Cont Lens Anterior Eye*. 2012;35:39-45.
37. Compañ V, Tiemblo P, García F, García JM, Guzmán J, Riande E. A Potentiostatic study of oxygen transport through poly(2-Ethoxyethyl methacrylate-Co-2,3-Dihydroxypropylmethacrylate) hydrogel membranes. *Biomaterials*. 2005;26:3783-3791.
38. Siegfried CJ, Shui YB, Holekamp NM, Bai F, Beebe DC. Oxygen distribution in the human eye: relevance to the etiology of open-angle glaucoma after vitrectomy. *Invest Ophthalmol Vis Sci*. 2010;51:5731-5738.
39. Lira M, Pereira C, Real Oliveira ME, Castanheira E. Importance of contact lens power and thickness in oxygen transmissibility. *Cont Lens Anterior Eye*. 2015;38:120-126.

## SUPPORTING INFORMATION

Additional supporting information can be found online in the Supporting Information section at the end of this article.

**How to cite this article:** Aguilera-Arzo M, Compañ V. A three-dimensional model to describe complete human corneal oxygenation during contact lens wear. *J Biomed Mater Res*. 2022;1-12. doi:[10.1002/jbm.b.35180](https://doi.org/10.1002/jbm.b.35180)